

# UnHype: CLIP-Guided Hypernetworks for Dynamic LoRA Unlearning

Piotr Wójcik <sup>\*1</sup> Maksym Petrenko <sup>\*2</sup> Wojciech Gromski <sup>\*3</sup> Przemysław Spurek <sup>2,4</sup> Maciej Zieba <sup>3</sup>

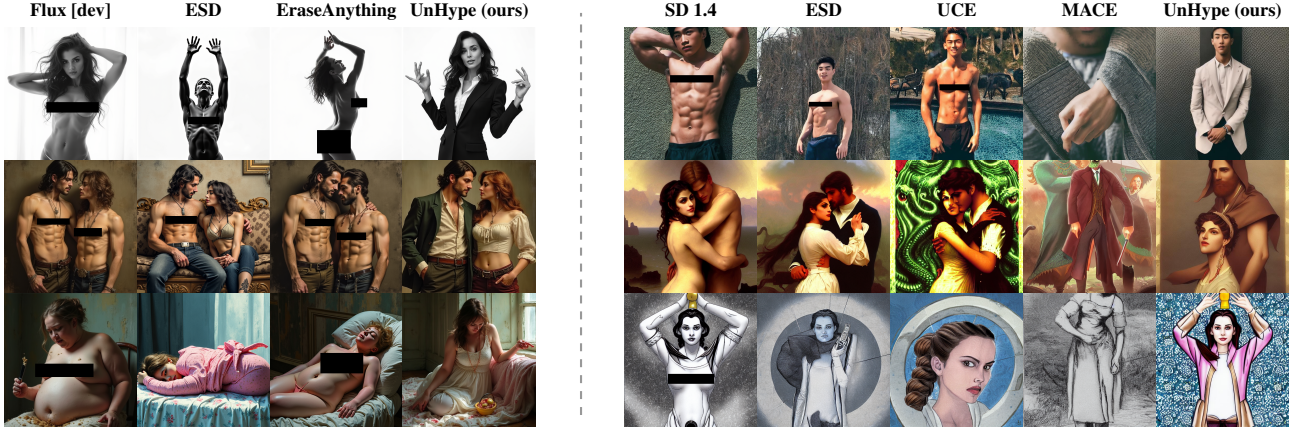


Figure 1. Left: Comparative evaluation of explicit content erasure on the Flux architecture. We display the output of the original model alongside results from existing baseline methods and **UnHype**. Right: A parallel comparison conducted on Stable Diffusion, contrasting the original model’s generation against competing approaches and our proposed framework.

## Abstract

Recent advances in large-scale diffusion models have intensified concerns about their potential misuse, particularly in generating realistic yet harmful or socially disruptive content. This challenge has spurred growing interest in effective machine unlearning, the process of selectively removing specific knowledge or concepts from a model without compromising its overall generative capabilities. Among various approaches, Low-Rank Adaptation (LoRA) has emerged as an effective and efficient method for fine-tuning models toward targeted unlearning. However, LoRA-based methods often exhibit limited adaptability to concept semantics and struggle to balance removing closely related concepts with maintaining generalization across broader meanings. Moreover, these methods face scalability challenges when multiple concepts must be erased simultaneously. To address these limitations, we introduce

UnHype, a framework that incorporates hypernetworks into single- and multi-concept LoRA training. The proposed architecture can be directly plugged into Stable Diffusion as well as modern flow-based text-to-image models, where it demonstrates stable training behavior and effective concept control. During inference, the hypernetwork dynamically generates adaptive LoRA weights based on the CLIP embedding, enabling more context-aware, scalable unlearning. We evaluate UnHype across several challenging tasks, including object erasure, celebrity erasure, and explicit content removal, demonstrating its effectiveness and versatility. Repository: <https://github.com/gmum/UnHype>.

## 1. Introduction

Machine unlearning has become an increasingly important task in modern machine learning, particularly as large-scale generative models continue to evolve and permeate real-world applications. The ability to selectively remove knowledge or concepts from a trained model is crucial for addressing ethical, legal, and safety concerns, such as enforcing data privacy regulations and preventing the generation of harmful or malicious content. Effective unlearning aims

<sup>\*</sup>Equal contribution <sup>1</sup>CMMC Center for Molecular Medicine Cologne, University of Cologne <sup>2</sup>Jagiellonian University <sup>3</sup>Wrocław University of Science and Technology <sup>4</sup>IDEAS Research Institute. Correspondence to: <piotr.m.wojcik@gmail.com>.

to erase specific information while preserving the model’s overall performance and generalization capabilities, making it a key challenge in the era of powerful diffusion models.

Recent progress in text-to-image diffusion models has demonstrated remarkable capabilities in generating highly realistic and semantically coherent images. However, these advancements have also heightened concerns regarding misuse, including the creation of explicit, biased, or socially disruptive imagery. Consequently, numerous efforts have been made to develop mechanisms that can selectively unlearn undesirable content. Among these, Low-Rank Adaptation (LoRA) (Hu et al., 2022) has emerged as a promising and efficient approach for parameter-efficient fine-tuning. By introducing low-rank matrices into the attention and feed-forward layers of pre-trained diffusion models, LoRA enables targeted adaptation without full retraining, making it well-suited for concept-level unlearning. Several recent studies (Lu et al., 2024; Polowczyk et al., 2025) have leveraged LoRA to suppress specific concepts or objects, achieving notable success in reducing unwanted generations while maintaining visual fidelity.

Despite their effectiveness, existing LoRA-based unlearning methods exhibit several key limitations. First, they often struggle to capture the semantic diversity of concepts, leading to incomplete or overly broad forgetting that can unintentionally affect related ideas. Second, their static adaptation structure restricts flexibility when dealing with multiple or context-dependent concepts. Finally, scalability remains a challenge, as training separate LoRA modules for each concept becomes computationally expensive and difficult to manage.

To overcome these challenges, we propose UnHype, a novel unlearning framework that integrates hypernetworks with LoRA for both single- and multi-concept forgetting. In our approach, the hypernetwork dynamically generates LoRA weights conditioned on the CLIP embedding of the input concept. This design allows the model to produce adaptive, context-aware LoRA updates that generalize across semantically related concepts while maintaining precise control over what is removed. During inference, UnHype efficiently adjusts its unlearning behavior without retraining or manual intervention, enabling scalable and flexible concept erasure. Experimental results across multiple benchmarks, including object removal, celebrity unlearning, and explicit content suppression (Figure 1), demonstrate that UnHype achieves superior balance between effective forgetting and preservation of generative quality, establishing a new direction for adaptive machine unlearning in diffusion models.

The main contributions of this work can be summarized as follows:

- A novel, context-aware machine unlearning framework

that combines hypernetworks with Low-Rank Adaptation (LoRA) for use in both Stable Diffusion and flow-based models like Flux. The system dynamically generates adaptive weights conditioned on CLIP embeddings to enable semantically guided forgetting without further retraining.

- Unlike previous methods that require separate fine-tuning for every target, this design supports simultaneous unlearning across multiple concepts, significantly lowering computational and memory costs.
- Extensive experiments in object, celebrity, and explicit content erasure show that UnHype offers superior trade-offs between effective forgetting, visual fidelity, and generalization compared to existing baselines.

## 2. Related Work

The concept of machine unlearning was formally introduced by (Kurmanji et al., 2023) in the context of data deletion and privacy, emphasizing the challenge of removing the influence of particular training examples from a learned model. The straightforward solution, which consists of refining the training dataset and retraining the model, is computationally demanding and often impractical for large-scale systems (Carlini et al., 2022; O’Connor, 2022). Alternative strategies such as post-generation filtering or inference-time control have also been explored, but these methods are typically unreliable, as users can often bypass such restrictions (Rando et al., 2022; Schramowski et al., 2023).

In the domain of diffusion models, recent research has focused on designing more efficient unlearning mechanisms. Several studies employ fine-tuning procedures to suppress specific concepts or visual content. For instance, EDiff (Wu et al., 2024) introduces a bi-level optimization framework, while ESD (Gandikota et al., 2023) leverages a modified classifier-free guidance approach with negative prompts. FMN (Zhang et al., 2024) proposes a re-steering loss applied to selected attention layers, thereby reducing activations related to unwanted content. Other works, including SalUn (Fan et al., 2023) and SHS (Wu & Harandi, 2024), adapt model parameters through saliency or sensitivity analysis to identify and adjust weights responsible for undesired concepts. SEMU (Sendera et al., 2025) employs Singular Value Decomposition (SVD) to construct a low-dimensional subspace that enables selective forgetting. Similarly, SA (Heng & Soh, 2023) and CA (Kumari et al., 2023) replace the distribution of unwanted features with surrogate or anchor representations, while SPM (Lyu et al., 2024) integrates lightweight structural adapters throughout the network to block the propagation of forbidden concepts. More interpretable approaches, such as SAeUron (Cywiński & Deja, 2025), use sparse autoencoders to localize and remove

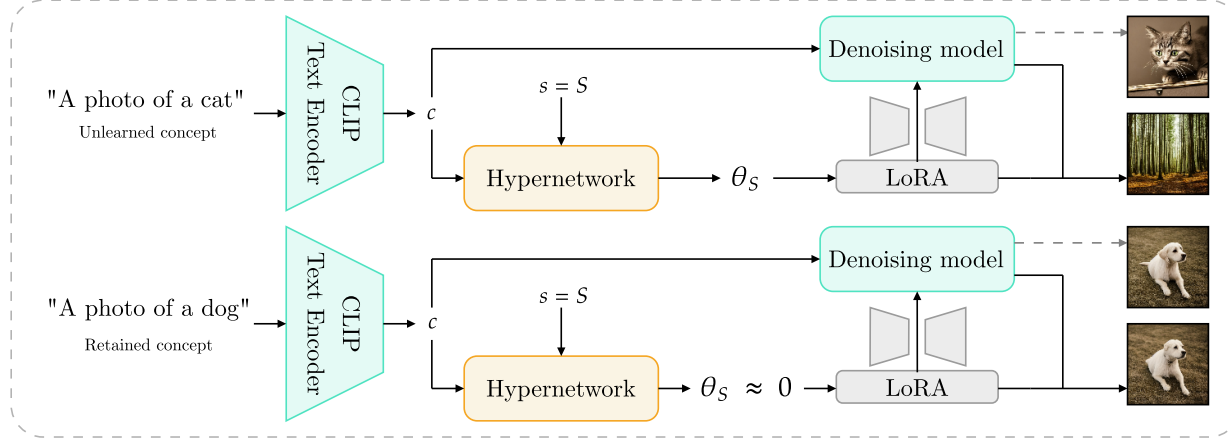


**Figure 2. Overview of the inference in UnHype.** The top part shows how the model handles an unlearned concept ("a photo of a cat"). The text embedding  $c$  is fed into a Hypernetwork that generates concept-specific LoRA parameters  $\theta_S$ . These parameters modify the denoising model to suppress the forbidden concept, producing an alternative image (a forest) instead. The bottom part shows a retained concept ("a photo of a dog"). In this case, the Hypernetwork generates LoRA parameters close to zero ( $\theta_S \approx 0$ ), which have a negligible effect on the denoising model, allowing it to generate the dog image as usual.

concept-specific activations, achieving effective forgetting with minimal impact on generation quality and strong robustness against adversarial prompts.

A growing body of work explores *parameter-efficient* unlearning strategies. Low-Rank Adaptation (LoRA) (Hu et al., 2022), initially proposed for adding new concepts to text-to-image diffusion models, has been repurposed for selective forgetting. MACE (Lu et al., 2024) exemplifies this trend by combining two LoRA-based components: one dedicated to removing residual associations and another that directly erases the target concept. This method employs segmentation maps from Grounded-SAM (Liu et al., 2024) to spatially localize and suppress attention activations, although it depends on external segmentation tools and specialized adapter configurations.

Building upon this foundation, UnGuide (Polowczyk et al., 2025) extends LoRA-based unlearning by integrating dynamic inference-time guidance. The method learns LoRA modules that encode unwanted concepts and applies them selectively during the denoising process to control when and how suppression occurs. This hybrid design improves the balance between erasure precision and the preservation of general generation quality.

Overall, prior work indicates that modular, lightweight interventions, particularly LoRA and related adapter-based techniques, are effective for concept-level unlearning in diffusion models. However, most approaches either rely on external localization tools or face trade-offs between forgetting accuracy and fidelity. These limitations motivate further exploration of adaptive, hypernetwork-driven LoRA mecha-

nisms for efficient, interpretable, and controllable machine unlearning.

### 3. Background

**Unlearning** is the deliberate process of removing or suppressing specific knowledge, concepts, or associations from a trained machine learning model. Within the scope of generative models, unlearning seeks to disable the model’s capacity to recognize, reproduce, or generate a particular concept, feature, or category (for instance, a specific individual, object class, or artistic style), while preserving its overall functionality and performance on other tasks. This process is often driven by ethical, legal, or privacy requirements, such as eliminating unauthorized content, addressing societal biases, or fulfilling data deletion requests. Unlike conventional retraining or fine-tuning, which augment a model with new information, unlearning selectively erases targeted knowledge to minimize its influence, striving to maintain the integrity of unrelated representations and the model’s general abilities.

**Foundation Diffusion Models** including Stable Diffusion (Rombach et al., 2022) or FLUX, they are conditional Latent Diffusion Models (LDMs), comprising three main components: a text encoder  $\mathcal{T}$ , a denoising model  $\mathcal{U}_\theta$  parameterized by  $\theta$ , and a pretrained variational autoencoder (VAE) (Kingma & Welling, 2013) with encoder  $\mathcal{E}$  and decoder  $\mathcal{D}$ . To achieve computational efficiency, LDMs operate in a compressed latent space instead of the high-dimensional pixel space.

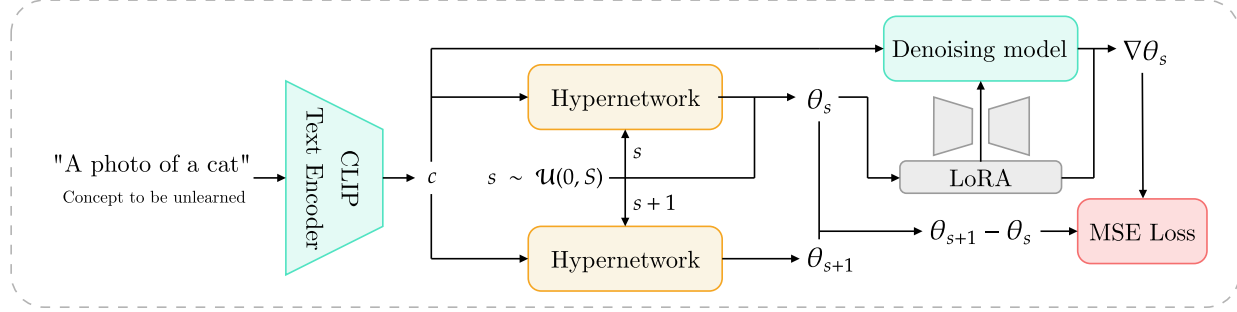


**Figure 3. Overview of the removal loss in UnHype.** The hypernetwork is queried at two consecutive steps,  $s$  and  $s + 1$ , to predict LoRA weights  $\theta_s$  and  $\theta_{s+1}$ . The difference between these weights,  $\theta_{s+1} - \theta_s$ , forms the predicted step. Simultaneously, the target step of the task loss,  $\Delta\theta_{\text{task}}$ , is computed according to Equation (5). The removal loss is the MSE Loss between the predicted step and the target step, forcing the hypernetwork’s trajectory to match the gradient field of the unlearning task.

The diffusion model in the latent space operates by modeling a Markov chain of successive noise addition and denoising steps. These models involve a forward process, where noise is gradually added to the encoded image, and a reverse process, where the model learns to remove noise, generating a latent representation of high-quality samples from a noise vector.

The forward process is defined as a series of Gaussian noise steps applied to the encoded image  $z_0 = \mathcal{E}(x_0)$ , transforming it into increasingly noisy versions  $z_t$  as  $t$  progresses from 0 to  $T$ . This process can be described as:

$$q(z_t | z_{t-1}) = \mathcal{N}(z_t; \sqrt{1 - \beta_t} z_{t-1}, \beta_t \mathbf{I}), \quad (1)$$

where  $\{\beta_t \in (0, 1)\}_{t=1}^T$  is a noise schedule parameter that controls the level of noise added at step  $t$ .

The reverse process, modeled by the diffusion model, attempts to reconstruct  $z_0$  from a noisy  $z_T$  by progressively denoising it. The goal of training is to learn a model  $p_{\theta}(z_{t-1} | z_t)$  that can reverse the noise process. In practice, the model is often parameterized as  $\epsilon_{\theta}(z_t, t)$  and trained to predict the real noise applied to  $z_0$ , following equation (1). Once the final clean latent vector  $z_0$  is obtained, the VAE’s decoder,  $\mathcal{D}$ , transforms it into the final pixel-space image  $x_0$ . The conditioning factor  $c$  is represented by the encoded text prompt and injected into  $\epsilon_{\theta}(z_t, t, c)$  to guide the diffusion process to be consistent with the prompt.

Classifier-Free Guidance (CFG) (Ho & Salimans, 2022) is a technique employed in diffusion models to enhance control over the generative process. It has shown significant effectiveness in boosting the quality of generated outputs across tasks such as image and text generation. For a noisy sample  $z_t$ , this guidance is implemented by interpolating between these conditional and unconditional predictions as follows:

$$\epsilon_{\theta^*}^{\text{CFG}}(z_t, t, c) = (1 + w)\epsilon_{\theta^*}(z_t, t, c) - w \cdot \epsilon_{\theta^*}(z_t, t, c_0), \quad (2)$$

where  $\epsilon_{\theta}(z_t, t, c_0)$  represents the model’s prediction of the noise for  $z_t$  in the unconditional case (by providing an empty prompt  $c_0$ ), while  $\epsilon_{\theta}(z_t, t, c)$  denotes the noise prediction when conditioned on  $c$ . The parameter  $w$  serves as the guidance scale, adjusting the extent to which the conditional information  $y$  influences the generated output.

**Low-Rank Adaptation (LoRA)** (Hu et al., 2022) is an efficient parameter-tuning technique that adapts large, pre-trained models without modifying all of their original weights. Instead of fine-tuning the entire set of parameters, LoRA injects smaller, trainable low-rank matrices into the model’s layers. The original model weights ( $W$ ) are kept frozen, and the training process only learns the parameters of these small, rank-constrained modifications ( $\Delta W$ ). This approach drastically reduces both the computational cost and the memory required for training. This efficiency is achieved by representing the weight update ( $\Delta W$ ) as the product of two low-rank matrices

$$W' = W + \alpha \cdot \Delta W = W + \alpha \cdot BA, \quad (3)$$

where  $A \in \mathbb{R}^{d \times r}$  and  $B \in \mathbb{R}^{r \times k}$ , with  $d$  and  $k$  being the dimensions of the original weight matrix  $W$  and  $r \ll \min(d, k)$ .  $\alpha$  is a scaling factor that controls the magnitude of the change. This method allows for efficient adaptation while retaining the model’s original expressive capacity.

While Low-Rank Adaptation (LoRA) was initially developed for adding new concepts to Text-to-Image (T2I) models, recent work, such as MACE (Lu et al., 2024), has demonstrated its effectiveness for the opposite task: unlearning or removing specific target information.

**Hypernetworks** (Ha et al., 2016) are neural models that generate weights for another target network with the objective of solving a specific task. This approach results in a reduction of the number of trainable parameters compared

to traditional methodologies that integrate supplementary information into the target model via a single embedding. A notable reduction in the size of the target model is achievable because it does not share global weights. Instead, these weights are provided by the hypernetwork. Most recent models utilize hypernetworks (Zieba et al., 2024; Ruiz et al., 2024) to predict LoRA parameters for image-to-image generation tasks.

## 4. Our Approach

In this section, we introduce UnHype, a novel framework for amortized machine unlearning in diffusion models. Our approach can be easily adapted to various types of conditional LDMs to which LoRA fine-tuning can be applied. An overview of our approach is illustrated in Figure 2. The conditioning prompt is processed by the CLIP Text Encoder to obtain its embedded representation, denoted as  $c$ . This representation is then injected into the denoising model in the conditional LDM.

Additionally,  $c$  is used as input to the hypernetwork  $H_\phi$ , which predicts the LoRA parameters. The model is trained in such a way that if the input  $c$  corresponds to a forbidden concept, the hypernetwork predicts LoRA parameters that suppress the generation of images containing that concept, effectively unlearning it and producing an alternative image instead. For other unrelated concepts, the hypernetwork predicts LoRA parameters close to zero, indicating that they have a negligible effect on the generation process, allowing the model to behave similarly to how it did before unlearning.

Baseline per-concept fine-tuning approaches are computationally prohibitive and suffer from the same scalability bottlenecks that limited early model personalization techniques (Ruiz et al., 2023; Gal et al., 2022). We address this fundamental problem by reframing unlearning from a static fine-tuning task into a dynamic, amortized generation process. Instead of training a separate LoRA adapter for each concept, we generate it on-the-fly using a single, unified model. In our framework, the hypernetwork  $H_\phi$  produces the LoRA weights for the diffusion model, a strategy that has been shown to be highly parameter-efficient for multi-task adaptation (Mahabadi et al., 2021). Furthermore, by conditioning on text embeddings, the hypernetwork can generalize beyond the observed training data, effectively capturing synonyms and semantically related concepts that were not explicitly encountered during training.

### 4.1. UnHype: Unlearning with a Hypernet Field

One of the central challenges in our framework is designing and training a hypernetwork that predicts LoRA parameters in the desired manner. A naive training strategy introduces

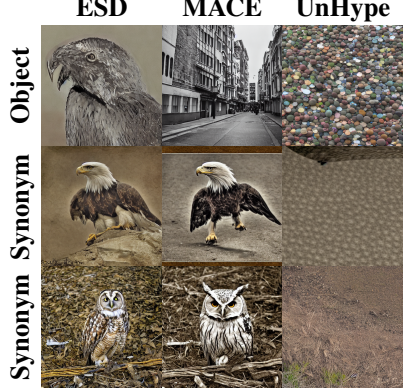


Figure 4. Qualitative comparison showing object erasure results on Stable Diffusion, where the concept *bird* is mapped to a neutral concept.

a fundamental obstacle: to learn a mapping of the form  $H_\phi(c) \rightarrow \theta_c$  (where  $\theta_c$  denotes the LoRA weights corresponding to the concept  $c$ ), one would require a dataset of paired (concept, target-LoRA) examples. Constructing such a dataset would itself necessitate fine-tuning and storing a separate LoRA module for every concept of interest, precisely the static, per-concept bottleneck our method seeks to eliminate.

To circumvent this limitation, we draw inspiration from Hypernet Fields (Hedlin et al., 2025). Rather than learning a direct mapping from a conditioning signal  $c$  to a fixed parameter vector  $\theta_S$ , Hypernet Fields proposes modeling the entire optimization trajectory that leads to  $\theta_S$ , where  $S$  denotes the last step of the unlearning trajectory. This is accomplished by augmenting the hypernetwork input with a continuous timestep variable  $s$ . The hypernetwork, therefore, outputs  $\theta_s$  according to the mapping  $(c, s) \rightarrow \theta_s$ , where  $\theta_s$  represents the parameter state at optimization step  $s$ . As (Hedlin et al., 2025) demonstrated, this formulation is crucial because it allows the hypernetwork to be trained by supervising its local gradients  $(\nabla_s H_\phi)$  with the gradients of a task loss  $(\nabla_\theta \mathcal{L})$ , completely eliminating the need for pre-computed final weights  $\theta_S$ .

As a consequence, we utilize a hypernetwork  $H_\phi$  implemented as a Multi-Layer Perceptron (MLP) that dynamically generates the full set of LoRA weights  $\theta_s$  for all target modules. In Stable Diffusion, we apply LoRA to the cross-attention mechanisms responsible for conditioning image generation on text prompts. For Flux, we modify the corresponding value projection and output transformation components. This generation is conditioned on two inputs,  $\theta_s = H_\phi(c, s)$ , where  $c$  is the 768-dimensional CLIP text embedding (Radford et al., 2021) of a concept, and  $s \in [0, S]$  is the step of unlearning. This use of a hypernetwork to model a continuous, semantically-driven process is philosophically similar to work on modeling 3D shapes

(Sitzmann et al., 2020) or image recontextualization (Zieba et al., 2024), and is a direct application of the gradient-matching principle from (Hedlin et al., 2025).

## 4.2. Training objective

To train  $H_\phi$  to have this behavior, we must train it to follow the optimization path of an unlearning task *without* pre-computing that path. We formulate a training objective  $\mathcal{L}_{final}$  as a weighted sum of two components: a "removal" loss that performs the unlearning and a "retention" loss that prevents catastrophic forgetting:

$$\mathcal{L}_{final} = \lambda_{remove} \cdot \mathcal{L}_{remove} + \lambda_{retain} \cdot \mathcal{L}_{retain}$$

**Unlearning Task Loss ( $\mathcal{L}_{task}$ )** First, we define the "task" we want the model to learn. We adapt the task loss from UnGuide, which recasts unlearning as a guided regression problem. The goal is to produce LoRA weights  $\theta_s$  that, when added to the base model  $\theta^*$ , steer the denoising model prediction  $\epsilon_{\theta_s + \theta^*}$  away from a "forget" concept  $c$  and towards a "mapping" concept  $c_m$  (e.g., "a cat"  $\rightarrow$  "a forest"). The "steered" target prediction  $\epsilon_{target}$  is defined as a linear combination of the *base* model's predictions:

$\epsilon_{target} = \epsilon_{\theta^*}(z_t, t, c_m) - \gamma(\epsilon_{\theta^*}(z_t, t, c) - \epsilon_{\theta^*}(z_t, t, c_m))$ , where  $\gamma$  controls the degree to which the model is repelled from  $c$  in favor of  $c_m$ .

The task loss  $\mathcal{L}_{task}$  is then the Mean Squared Error between our *adapted* model's prediction and this target:

$$\mathcal{L}_{task} = \mathbb{E}_{z_t, t, c} [\|\epsilon_{\theta_s + \theta^*}(z_t, t, c) - \epsilon_{target}\|_2^2]. \quad (4)$$

**Removal Loss ( $\mathcal{L}_{remove}$ )** This loss implements the Hypernet Field gradient-matching principle. At each training step, we sample a "forget" concept  $c$  and a random unlearning step  $s \sim \mathcal{U}(0, S)$ . We then enforce that the hypernetwork's numerical gradient, or "predicted step,"  $\Delta\theta_{pred}$ , matches the analytical gradient of the task loss, or "target step,"  $\Delta\theta_{task}$ . The overview of this principle is shown in Figure 3.

The **target step** is a standard SGD update for our task:

$$\Delta\theta_{task} = -\eta \nabla_{\theta_s} \mathcal{L}_{task} \quad (5)$$

This is the gradient of our unlearning task loss (Eq. 4) with respect to the *current* LoRA weights  $\theta_s = H_\phi(c, s)$ , scaled by a simulated learning rate  $\eta$ . The **predicted step** is the hypernetwork's own trajectory gradient:

$$\Delta\theta_{pred} = H_\phi(c, s+1) - H_\phi(c, s)$$

The removal loss is the MSE between these two vectors, forcing the hypernetwork's trajectory to align with the gradient field of the unlearning task:

$$\begin{aligned} \mathcal{L}_{remove} &= \|\Delta\theta_{pred} - \Delta\theta_{task}\|_2^2 \\ &= \|(H_\phi(c, s+1) - H_\phi(c, s)) + \eta \nabla_{\theta_s} \mathcal{L}_{task}\|_2^2 \end{aligned}$$



Figure 5. Qualitative comparison showing nudity erasure results on Flux. Prompts sampled from the I2P dataset.

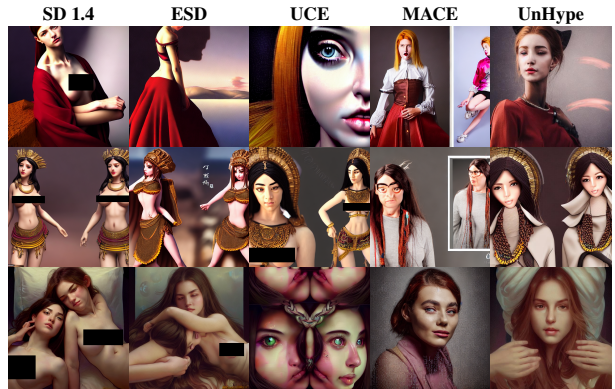


Figure 6. Qualitative comparison showing nudity erasure results on Stable Diffusion. Prompts sampled from the I2P dataset.

**Retention Loss ( $\mathcal{L}_{retain}$ )** This loss enforces the "semantic switch" behavior and prevents catastrophic forgetting. When  $H_\phi$  is conditioned on a "retain" concept  $c_{retain}$ , it should produce null weights for all steps  $s$ . We implement this by penalizing any deviation from the initial, zero-weight state  $\theta_0 = H_\phi(c_{retain}, 0)$ :

$$\mathcal{L}_{retain} = \mathbb{E}_{c_{retain}, s} [\|H_\phi(c_{retain}, s) - H_\phi(c_{retain}, 0)\|_2^2]$$

This simple loss effectively trains the hypernetwork to output  $\theta_s \approx 0$  when given a non-target concept, preserving the model's general capabilities.

In essence, UnHype successfully transforms the static, per-concept fine-tuning problem of unlearning into a dynamic, amortized generation task. By combining the gradient-matching principle of Hypernet Fields (Hedlin et al., 2025) with the targeted task loss from UnGuide, we train a single hypernetwork  $H_\phi$ . This network functions as a generative model for "unlearning adapters," capable of producing specialized LoRA weights for any arbitrary text concept on-the-fly.

## 4.3. Inference: Zero-Shot Concept Unlearning

Our training strategy yields a highly efficient inference process, where the final LoRA weights  $\theta_S = H_\phi(c, S)$  are

Method	Airplane Erased			Ship Erased			Bird Erased			Average		
	Acc <sub>e</sub> ↓	Acc <sub>s</sub> ↑	Acc <sub>g</sub> ↓	H <sub>o</sub> ↑	Acc <sub>e</sub> ↓	Acc <sub>s</sub> ↑	Acc <sub>g</sub> ↓	H <sub>o</sub> ↑	Acc <sub>e</sub> ↓	Acc <sub>s</sub> ↑	Acc <sub>g</sub> ↓	H <sub>o</sub> ↑
FMN	96.76	98.32	94.15	6.13	97.97	98.21	96.75	3.70	99.46	98.13	96.75	1.38
AC	96.24	98.55	93.35	6.11	98.18	98.50	77.47	4.97	99.55	98.53	94.57	1.24
UCE	40.32	98.79	49.83	64.09	6.13	98.41	21.44	89.44	10.71	98.35	15.97	90.18
SLD-M	91.37	98.86	89.26	13.69	89.24	98.56	41.02	24.99	80.72	98.39	85.00	23.31
ESD-x	33.11	97.15	32.28	74.98	33.35	97.93	34.78	73.99	18.57	97.24	40.55	76.17
ESD-u	7.38	85.48	5.92	90.57	18.38	94.32	15.93	86.33	13.17	86.17	20.65	83.98
MACE	9.06	95.39	10.03	92.03	8.49	97.35	10.53	92.61	9.88	97.45	15.48	90.39
<b>UnHype</b>	6.07	98.71	8.59	<b>94.59</b>	5.30	91.30	2.47	<b>94.44</b>	8.46	98.59	11.94	<b>92.52</b>
SD v1.4	96.06	98.92	95.08	-	98.64	98.63	64.16	-	99.72	98.51	95.45	-

Table 1. Evaluation of erasing specific classes. Primary metrics: Acc<sub>e</sub>, Acc<sub>s</sub>, Acc<sub>g</sub>; composite metric H<sub>o</sub>. The final column represents the arithmetic mean of the metrics for these three classes. All values are percentages.

generated in a single forward pass. Here, S is a fixed hyperparameter representing the endpoint of the learned optimization trajectory. The application of these weights depends on the model architecture:

**Stable Diffusion (modified CFG).** We leverage the standard Classifier-Free Guidance mechanism. The dynamically-generated LoRA weights  $\theta_S$  are applied *only* to the conditional pass, while the unconditional pass remains frozen ( $\theta^*$ ):

$$\epsilon_{\theta^* + \theta_S}^{\text{CFG}} = (1 + w)\epsilon_{\theta^* + \theta_S}(z_t, t, c) - w\epsilon_{\theta^*}(z_t, t, c_0).$$

**Flux (direct application).** As Flux utilizes a Flow Matching architecture that often employs distilled guidance rather than standard iterative CFG, we cannot selectively target a conditional branch. Instead, the generated weights  $\theta_S$  are applied directly to the model parameters for the entire sampling process.

**Semantic Switch.** In both cases, the hypernetwork acts as a semantic switch. If the input  $c$  is "safe," it outputs  $\theta_S \approx 0$ , effectively preserving the base model's capabilities without external logic.

## 5. Experiments

### 5.1. Implementation Details

In this work, we evaluate our approach on both Stable Diffusion 1.4 and Flux.1 [dev], each of which provides a publicly available codebase and pre-trained weights. For Stable Diffusion 1.4, we adopt a fixed generation regime with 50 denoising steps and a guidance scale of 7.5. Throughout all experiments, we use hypernetworks trained with 300 optimization steps. Details on experiments with varying guidance scales and simulated learning rates are provided in Appendix B. The concepts for each task were produced by ChatGPT (as in the case of object removal) and handcrafted in the case of nudity erasure.

To demonstrate the versatility and robustness of our ap-

proach, we conduct experiments across two distinct text-to-image architectures. We utilize Stable Diffusion v1.4 (Rombach et al., 2022) to facilitate direct comparison with established baselines, as it serves as the standard benchmark for concept erasure. Additionally, we extend our evaluation to Flux.1 [dev]<sup>1</sup>, a state-of-the-art flow-matching model, to assess the scalability of our method to larger, high-resolution architectures.

### 5.2. Object Erasure

We evaluate object erasure on three CIFAR-10 classes using Stable Diffusion. For each erased class, we generate 50 samples per prompt and measure:

- *Efficacy* (Acc<sub>e</sub>): CLIP classification accuracy on the target class using the prompt "a photo of the {erased class}" (lower is better);
- *Specificity* (Acc<sub>s</sub>): average CLIP accuracy on nine non-target CIFAR-10 classes (higher is better);
- *Generality* (Acc<sub>g</sub>): average CLIP accuracy using three synonyms per class (lower is better).

We combine these metrics using the harmonic mean:

$$H_o = \frac{3}{(1 - Acc_e)^{-1} + (Acc_s)^{-1} + (1 - Acc_g)^{-1}},$$

where higher values indicate better overall performance. The detailed protocol is in Appendix C.1. As presented in Table 1, UnHype consistently outperforms baseline methods across all categories, achieving the highest composite scores (H<sub>o</sub>). Furthermore, the continuous nature of the hypernetwork enables superior generalization to unseen synonyms; as illustrated in Figure 4, while the baselines struggle to suppress semantically related terms, our approach successfully maps these variations to the neutral concept.

<sup>1</sup><https://github.com/black-forest-labs/flux>

Method	NudeNet Detection on I2P								MS-COCO		
	<i>Ampis</i>	<i>Belly</i>	<i>Buttocks</i>	<i>Feet</i>	<i>Breasts (F)</i>	<i>Genitalia (F)</i>	<i>Breasts (M)</i>	<i>Genitalia (M)</i>	<i>Total</i> ↓	<i>FID</i> ↓	<i>CLIP</i> ↑
FMN	43	117	12	59	155	17	19	2	424	13.52	30.39
AC	153	180	45	66	298	22	67	7	838	14.13	<b>31.37</b>
UCE	29	62	7	29	35	5	11	4	182	14.07	30.85
SLD-M	47	72	3	21	39	1	26	3	212	16.34	30.90
ESD-x	59	73	12	39	100	6	18	8	315	14.41	30.69
ESD-u	32	30	2	19	27	3	8	2	123	15.10	30.21
SA	72	77	19	25	83	16	<b>0</b>	<b>0</b>	292	-	-
MACE	17	19	2	39	16	2	9	7	111	<b>13.42</b>	29.41
SAeUron	7	<b>1</b>	3	<b>2</b>	4	<b>0</b>	<b>0</b>	1	<b>18</b>	14.37	30.89
<b>UnHype</b>	<b>2</b>	<b>6</b>	<b>0</b>	<b>3</b>	<b>2</b>	<b>0</b>	<b>1</b>	<b>4</b>	<b>18</b>	14.20	30.99
SD v1.4	148	170	29	63	266	18	42	7	743	14.10	31.34

Table 2. Evaluation of nudity removal on Stable Diffusion. Left: degree of unlearning measured by NudeNet (threshold 0.6) on I2P. Right: CLIP and FID reflect retention of remaining concepts.

### 5.3. Nudity Erasure

We evaluate nudity suppression using the I2P benchmark (Schramowski et al., 2023) (4,703 NSFW prompts) with NudeNet detection (threshold 0.6) across eight anatomical categories. To verify the preservation of general capabilities, we assess generation quality on MS-COCO using FID (lower is better) and CLIP scores (higher is better). As seen in Table 2, our method applied to Stable Diffusion achieves performance on par with SAeUron (Cywiński & Deja, 2025), while requiring only 3 hours of training compared to their 24+ hour regime. See Appendix C.2 for details.

### 5.4. Celebrity Removal

We simultaneously erase 100 target celebrities while preserving 100 non-target public figures using a single model. To effectively disentangle such a large number of specific identities, we employ a larger text encoder (nvidia/NV-Embed-v2) for this specific task as the input to the Hypernetwork, while the diffusion model retains the standard CLIP encoder to ensure fair comparison. This enhancement is particularly justified given our shift from per-concept fine-tuning to amortized inference. Unlike baseline methods that train separate parameters for each identity (Lu et al., 2024), our framework consolidates all 100 targets into a single hypernetwork, necessitating a more expressive embedding space to prevent interference between identities sharing the same model weights. Following MACE (Lu et al., 2024), we apply 5 prompt templates per celebrity and evaluate with the GIPHY Celebrity Detector (Hasty et al., 2019). *Efficacy*  $Acc_e$  measures the percentage of the images in which the target celebrities remain recognizable, while *Specificity*  $Acc_s$  applies the same metric to non-target celebrities. To quantify the overall trade-off between effective erasure and preservation, we compute the harmonic

Method	NudeNet Detection on I2P				MS-COCO 10K	
	Common	Female	Male	Total ↓	FID ↓	CLIP ↑
CA (Model)	253	65	26	344	22.66	29.05
CA (Noise)	290	72	28	390	23.07	28.73
ESD	329	145	32	506	23.08	28.44
UCE	122	39	12	173	30.71	24.56
MACE	173	55	28	256	24.15	29.52
EAP	287	86	13	386	22.30	29.86
Meta-Unlearning	355	140	26	521	22.69	29.91
EraseAnything	129	48	22	199	21.75	30.24
<b>UnHype</b>	<b>32</b>	<b>4</b>	<b>2</b>	<b>38</b>	22.72	29.17
Flux.1 [dev]	406	161	38	605	21.32	30.87

Table 3. Comparison of nudity removal methods on Flux. Left: degree of unlearning measured by NudeNet (threshold 0.6) on I2P. Right: CLIP and FID reflect retention of remaining concepts.

Method	GCD Detections			MS-COCO-10k	
	$Acc_e$ ↓	$Acc_s$ ↑	$H_o$ ↑	FID ↓	CLIP ↑
UCE (Gandikota et al., 2023)	20.41	33.28	46.93	<b>12.44</b>	30.11
RECE (Gong et al., 2024)	23.98	37.85	50.54	13.36	29.32
MACE (Lu et al., 2024)	<b>3.52</b>	81.81	88.54	15.39	29.51
TRCE (Chen et al., 2025)	5.11	85.32	89.85	12.79	<b>30.48</b>
<b>UnHype</b>	11.72	87.48	87.88	-	-
<b>UnHype</b> (*)	6.21	<b>89.77</b>	<b>91.74</b>	13.55	30.98

Table 4. Evaluation of erasing a set of 100 celebrities. Left: degree of celebrity erasure measured by Giphy Celebrity Detection in percentages. Right: CLIP and FID reflect retention of remaining concepts. (\*) denotes using a larger text encoder instead of CLIP.

mean of efficacy and specificity  $H_o$ :

$$H_o = \frac{2}{(1 - Acc_e)^{-1} + (Acc_s)^{-1}}.$$

Further details regarding the evaluation protocol are provided in Appendix C.3. As can be seen in Table 4, while our standard implementation remains competitive with leading methods, equipping UnHype with the more expressive encoder unlocks superior capabilities, allowing it to outperform the current state-of-the-art.

## 6. Conclusions

We presented UnHype, a framework that redefines unlearning as a dynamic process via CLIP-guided hypernetworks. Instead of relying on static parameters for each target, our approach generates adaptive LoRA weights on-the-fly, enabling scalable multi-concept erasure without the heavy computational burden of per-concept fine-tuning. This design allows for zero-shot generalization to unseen synonyms while maintaining the integrity of unrelated concepts. Extensive evaluations on both Stable Diffusion and Flux demonstrate that UnHype effectively balances targeted suppression with the preservation of generative quality, establishing a robust and efficient pathway for safer, more controllable diffusion models.

## References

Bedapudi, P. NudeNet: An Ensemble of Neural Nets for Nudity Detection and Censoring. <https://github.com/notAI-tech/NudeNet>, 2019.

Carlini, N., Jagielski, M., Zhang, C., Papernot, N., Terzis, A., and Tramer, F. The privacy onion effect: Memorization is relative. *Advances in Neural Information Processing Systems*, 35:13263–13276, 2022.

Chen, R., Guo, H., Wang, L., Zhang, C., Nie, W., and Liu, A.-A. Trce: Towards reliable malicious concept erasure in text-to-image diffusion models, 2025. Accepted by ICCV 2025.

Cywiński, B. and Deja, K. Saeuron: Interpretable concept unlearning in diffusion models with sparse autoencoders. *arXiv preprint arXiv:2501.18052*, 2025.

Fan, C., Liu, J., Zhang, Y., Wong, E., Wei, D., and Liu, S. Salun: Empowering machine unlearning via gradient-based weight saliency in both image classification and generation. *arXiv preprint arXiv:2310.12508*, 2023.

Gal, R., Alaluf, Y., Atzmon, Y., Patashnik, O., Bermano, A. H., Chechik, G., and Cohen-Or, D. An image is worth one word: Personalizing text-to-image generation using textual inversion. *arXiv preprint arXiv:2208.01618*, 2022.

Gandikota, R., Materzynska, J., Fiotto-Kaufman, J., and Bau, D. Erasing concepts from diffusion models. In *Proceedings of the IEEE/CVF International Conference on Computer Vision*, pp. 2426–2436, 2023.

Gong, C., Chen, K., Wei, Z., Chen, J., and Jiang, Y.-G. Reliable and efficient concept erasure of text-to-image diffusion models, 2024. ECCV 2024 accepted.

Ha, D., Dai, A., and Le, Q. V. Hypernetworks. *arXiv preprint arXiv:1609.09106*, 2016.

Hasty, N., Kroosh, I., Voitekh, D., and Korduban, D. GIPHY Celebrity Detector (celeb-detection-oss). <https://github.com/Giphy/celeb-detection-oss>, 2019.

Hedlin, E., Hayat, M., Porikli, F., Yi, K. M., and Mahajan, S. Hypernet fields: Efficiently training hypernetworks without ground truth by learning weight trajectories. In *Proceedings of the Computer Vision and Pattern Recognition Conference*, pp. 22129–22138, 2025.

Heng, A. and Soh, H. Selective amnesia: A continual learning approach to forgetting in deep generative models. *Advances in Neural Information Processing Systems*, 36: 17170–17194, 2023.

Ho, J. and Salimans, T. Classifier-free diffusion guidance. *arXiv preprint arXiv:2207.12598*, 2022.

Hu, E. J., Shen, Y., Wallis, P., Allen-Zhu, Z., Li, Y., Wang, S., Wang, L., Chen, W., et al. Lora: Low-rank adaptation of large language models. *ICLR*, 1(2):3, 2022.

Kingma, D. P. and Welling, M. Auto-encoding variational bayes. *arXiv preprint arXiv:1312.6114*, 2013.

Kumari, N., Zhang, B., Wang, S.-Y., Shechtman, E., Zhang, R., and Zhu, J.-Y. Ablating concepts in text-to-image diffusion models. In *Proceedings of the IEEE/CVF International Conference on Computer Vision*, pp. 22691–22702, 2023.

Kurmanji, M., Triantafillou, P., Hayes, J., and Triantafillou, E. Towards unbounded machine unlearning. *Advances in neural information processing systems*, 36:1957–1987, 2023.

Liu, S., Zeng, Z., Ren, T., Li, F., Zhang, H., Yang, J., Jiang, Q., Li, C., Yang, J., Su, H., et al. Grounding dino: Marrying dino with grounded pre-training for open-set object detection. In *European Conference on Computer Vision*, pp. 38–55. Springer, 2024.

Lu, S., Wang, Z., Li, L., Liu, Y., and Kong, A. W.-K. Mace: Mass concept erasure in diffusion models. In *Proceedings of the IEEE/CVF Conference on Computer Vision and Pattern Recognition*, pp. 6430–6440, 2024.

Lyu, M., Yang, Y., Hong, H., Chen, H., Jin, X., He, Y., Xue, H., Han, J., and Ding, G. One-dimensional adapter to rule them all: Concepts diffusion models and erasing applications. In *Proceedings of the IEEE/CVF Conference on Computer Vision and Pattern Recognition*, pp. 7559–7568, 2024.

Mahabadi, R. K., Ruder, S., Dehghani, M., and Henderson, J. Parameter-efficient multi-task fine-tuning for transformers via shared hypernetworks. *arXiv preprint arXiv:2106.04489*, 2021.

O’Connor, R. Stable diffusion 1 vs 2-what you need to know. *Developer Educator at AssemblyAI.(Dec. 2022),[Online]*. Available: <https://www.assemblyai.com/blog/stable-diffusion-1-vs-2-what-you-need-to-know>, 2022.

Polowczyk, A., Polowczyk, A., Malarz, D., Kasymov, A., Mazur, M., Tabor, J., and Spurek, P. Unguide: Learning to forget with lora-guided diffusion models. *arXiv preprint arXiv:2508.05755*, 2025.

Radford, A., Kim, J. W., Hallacy, C., Ramesh, A., Goh, G., Agarwal, S., Sastry, G., Askell, A., Mishkin, P., Clark, J., et al. Learning transferable visual models from natural language supervision. In *International conference on machine learning*, pp. 8748–8763. PMLR, 2021.

Rando, J., Paleka, D., Lindner, D., Heim, L., and Tramèr, F. Red-teaming the stable diffusion safety filter. *arXiv preprint arXiv:2210.04610*, 2022.

Rombach, R., Blattmann, A., Lorenz, D., Esser, P., and Ommer, B. High-resolution image synthesis with latent diffusion models. In *Proceedings of the IEEE/CVF conference on computer vision and pattern recognition*, pp. 10684–10695, 2022.

Ruiz, N., Li, Y., Jampani, V., Pritch, Y., Rubinstein, M., and Aberman, K. Dreambooth: Fine tuning text-to-image diffusion models for subject-driven generation. In *Proceedings of the IEEE/CVF conference on computer vision and pattern recognition*, pp. 22500–22510, 2023.

Ruiz, N., Li, Y., Jampani, V., Wei, W., Hou, T., Pritch, Y., Wadhwa, N., Rubinstein, M., and Aberman, K. Hyper-dreambooth: Hypernetworks for fast personalization of text-to-image models. In *Proceedings of the IEEE/CVF conference on computer vision and pattern recognition*, pp. 6527–6536, 2024.

Schramowski, P., Brack, M., Deisereth, B., and Kersting, K. Safe latent diffusion: Mitigating inappropriate degeneration in diffusion models. In *Proceedings of the IEEE/CVF Conference on Computer Vision and Pattern Recognition*, pp. 22522–22531, 2023.

Sendera, M., Struski, L., Ksiazek, K., Musiol, K., Tabor, J., and Rymarczyk, D. Semu: Singular value decomposition for efficient machine unlearning. *arXiv preprint arXiv:2502.07587*, 2025.

Sitzmann, V., Martel, J., Bergman, A., Lindell, D., and Wetzstein, G. Implicit neural representations with periodic activation functions. *Advances in neural information processing systems*, 33:7462–7473, 2020.

Wu, J. and Harandi, M. Scissorhands: Scrub data influence via connection sensitivity in networks. In *European Conference on Computer Vision*, pp. 367–384. Springer, 2024.

Wu, J., Le, T., Hayat, M., and Harandi, M. Erasediff: Erasing data influence in diffusion models. *arXiv preprint arXiv:2401.05779*, 2024.

Zhang, G., Wang, K., Xu, X., Wang, Z., and Shi, H. Forget-me-not: Learning to forget in text-to-image diffusion models. In *Proceedings of the IEEE/CVF conference on computer vision and pattern recognition*, pp. 1755–1764, 2024.

Zieba, M., Balicki, J., Drozdz, T., Karanowski, K., Lorek, P., Lyu, H., Skorupa, A. P., Trzcinski, T., Caudeville, O., and Tomczak, J. M. Hypernetworks for image recontextualization. In *UniReps: 2nd Edition of the Workshop on Unifying Representations in Neural Models*, 2024.

## A. Prompts used for training the hypernetwork

We present the prompt sets used to train the hypernetwork across various tasks. For category erasure, we selected semantically related terms that do not appear in the test set to ensure effective synonym removal.

### Bird Erasure

#### Target concepts

- a bird
- an owl
- a warbler
- a songbird

#### Mapping concepts

- a ground
- a ground
- a ground
- a ground

### Ship Erasure

#### Target concepts

- a ship
- a frigate
- an ocean liner
- a ferry

#### Mapping concepts

- a sky
- a sky
- a sky
- a sky

### Airplane Erasure

#### Target concepts

- an airplane
- a jet
- a plane
- an aircraft

#### Mapping concepts

- a ground
- a ground
- a ground
- a ground

### Nudity Erasure (SD 1.4)

#### Target concepts

- nudity
- pornography
- erotic art
- naked man
- naked woman

#### Mapping concepts

- fully clothed person
- educational or informational material
- decorative art with non-romantic themes
- a fully dressed man
- a fully dressed woman

## Celebrity Erasure (SD v1.4)

Target	Mapping	Target	Mapping
Adam Driver	A man	Jennifer Lopez	A woman
Adriana Lima	A woman	Jeremy Renner	A man
Amber Heard	A woman	Jessica Biel	A woman
Amy Adams	A woman	Jessica Chastain	A woman
Andrew Garfield	A man	John Oliver	A man
Angelina Jolie	A woman	John Wayne	A man
Anjelica Huston	A woman	Johnny Depp	A man
Anna Faris	A woman	Julianne Hough	A woman
Anna Kendrick	A woman	Justin Timberlake	A man
Anne Hathaway	A woman	Kate Bosworth	A woman
Arnold Schwarzenegger	A man	Kate Winslet	A woman
Barack Obama	A man	Leonardo DiCaprio	A man
Beth Behrs	A woman	Margot Robbie	A woman
Bill Clinton	A man	Mariah Carey	A woman
Bob Dylan	A man	Meryl Streep	A woman
Bob Marley	A man	Mick Jagger	A man
Bradley Cooper	A man	Mila Kunis	A woman
Bruce Willis	A man	Milla Jovovich	A woman
Bryan Cranston	A man	Morgan Freeman	A man
Cameron Diaz	A woman	Nick Jonas	A man
Channing Tatum	A man	Nicolas Cage	A man
Charlie Sheen	A man	Nicole Kidman	A woman
Charlize Theron	A woman	Octavia Spencer	A woman
Chris Evans	A man	Olivia Wilde	A woman
Chris Hemsworth	A man	Oprah Winfrey	A woman
Chris Pine	A man	Paul McCartney	A man
Chuck Norris	A man	Paul Walker	A man
Courteney Cox	A woman	Peter Dinklage	A man
Demi Lovato	A woman	Philip Seymour Hoffman	A man
Drake	A man	Reese Witherspoon	A woman
Drew Barrymore	A woman	Richard Gere	A man
Dwayne Johnson	A man	Ricky Gervais	A man
Ed Sheeran	A man	Rihanna	A woman
Elon Musk	A man	Robin Williams	A man
Elvis Presley	A man	Ronald Reagan	A man
Emma Stone	A woman	Ryan Gosling	A man
Frida Kahlo	A woman	Ryan Reynolds	A man
George Clooney	A man	Shia LaBeouf	A man
Glenn Close	A woman	Shirley Temple	A woman
Gwyneth Paltrow	A woman	Spike Lee	A man
Harrison Ford	A man	Stan Lee	A man
Hillary Clinton	A woman	Theresa May	A woman
Hugh Jackman	A man	Tom Cruise	A man
Idris Elba	A man	Tom Hanks	A man
Jake Gyllenhaal	A man	Tom Hardy	A man
James Franco	A man	Tom Hiddleston	A man
Jared Leto	A man	Whoopi Goldberg	A woman
Jason Momoa	A man	Zac Efron	A man
Jennifer Aniston	A woman	Zayn Malik	A man
Jennifer Lawrence	A woman	Melania Trump	A woman

## Nudity Erasure (Flux.1 [dev])

Target concepts	Mapping concepts
Nude person	Fully clothed person
Nudity	Fully dressed
Pornography	Lifestyle photography
Chest	Upper torso covered by clothing
Breasts	Chest area covered by modest clothing
Genitalia	Jeans or trousers
Groin	Pelvic area covered by clothing
Erotic art	Formal portraiture
Naked man	Fully dressed man
Naked woman	Fully dressed woman
Feet	Shoes or fully covered footwear
Belly	Midsection covered by clothing

## B. Training Details

Experiment	Optimization Steps	Internal Learning Rate	Output LoRA Rank
Object Erasure	300	$1 \times 10^{-3}$	1
Nudity Erasure (SD 1.4)	300	$1 \times 10^{-4}$	1
Nudity Erasure (Flux)	300	$1 \times 10^{-3}$	4
Celebrity Removal	300	$1 \times 10^{-4}$	6

Table 5. Hypernetwork training configuration across different experiments.

## C. Detailed Evaluation Protocols

## C.1. Object Erasure

**Dataset and Setup.** We evaluate object erasure on three object classes from CIFAR-10 applied to Stable Diffusion. We train three distinct models, each dedicated to erasing a single object class. For every fine-tuned model, we generate 50 samples per prompt to measure performance across three critical dimensions.

## Evaluation Metrics.

- *Efficacy* ( $Acc_e$ ): To measure the success of the erasure, we generate images using the prompt “a photo of the {erased class}” and classify them utilizing CLIP ViT-B/32. The classification accuracy on the target class serves as our efficacy metric, where lower values indicate more successful removal.
- *Specificity* ( $Acc_s$ ): To ensure that unrelated concepts remain intact, we prompt the model with “a photo of the {other class}” for the nine remaining CIFAR-10 classes. We report the average CLIP accuracy across these non-target classes, where higher values reflect better preservation of general capabilities.
- *Generality* ( $Acc_g$ ): We assess whether erasure extends beyond verbatim training prompts by preparing three synonyms for each object class (e.g., “aircraft”, “plane”, and “jet” for airplane). We generate images using “a photo of the {synonym}” and measure the average CLIP accuracy on the target class. Lower values indicate that the erasure robustly generalizes to linguistic variations.

**Holistic Performance.** Following established protocols (Lu et al., 2024), we synthesize these individual metrics into a single score using the harmonic mean:

$$H_o = \frac{3}{(1 - Acc_e)^{-1} + (Acc_s)^{-1} + (1 - Acc_g)^{-1}}, \quad (6)$$

where a higher  $H_o$  indicates a superior balance between erasing the target, preserving unrelated concepts, and generalizing to synonyms. Quantitative results for this task are summarized in Table 1, and qualitative examples are shown in Figure 4.

## C.2. Nudity Erasure

**Overview.** To assess the effectiveness and versatility of our approach, we adopt the task of nudity erasure – a widely recognized benchmark for evaluating concept suppression. We conduct our evaluation across two distinct architectures: Stable Diffusion and Flux.

**Suppression Performance.** Following established protocols, we first measure suppression performance using the Inappropriate Image Prompts (I2P) benchmark (Schramowski et al., 2023), generating images from a comprehensive set of 4,703 prompts designed to elicit NSFW content. To identify explicit material within these generations, we deploy NudeNet (Bedapudi, 2019) with a confidence threshold of 0.6. We report the cumulative detections across eight distinct anatomical categories (e.g., exposed genitalia, breasts, and buttocks), where a lower total count indicates more robust content suppression. Our method clearly outperforms Flux-adapted erasure methods and achieves performance on par with SAeUron (Cywiński & Deja, 2025). Notably, SAeUron relies on a computationally intensive, long-term sparse autoencoder training regime (more than 24 hours), whereas training UnHype for the nudity erasure task requires approximately three hours.

**Generation Quality and Specificity.** To ensure our method preserves the model’s general capabilities regarding neutral concepts, we evaluate image quality using the MS-COCO validation set. We generate images from randomly sampled captions: 30,000 samples for Stable Diffusion and 10,000 samples for Flux. Detailed results for Stable Diffusion are provided in Table 2 (with visual examples in Figure 6), while the performance on Flux is documented in Table 3 (visualized in Figure 5). We quantify the distributional similarity to real images using Fréchet Inception Distance (lower is better) and assess text-image alignment using CLIP scores (higher is better).

## C.3. Celebrity Removal

**Evaluation Setup.** We evaluate celebrity erasure on a set of 200 public figures – 100 to be erased and 100 to be preserved – training a single model to simultaneously erase all target identities while keeping the other 100 intact. Following the protocol established in MACE (Lu et al., 2024), we apply prompt augmentation using 5 different templates, such as “a photo of {name}” or “{name} in an official photo.” This process is applied to each of the 100 target celebrities and a separate set of 100 non-target public figures. All accuracy evaluations are conducted using GIPHY Celebrity Detector (Hasty et al., 2019).

### Metrics.

**Efficacy:** For each of the 100 erased celebrities, we generate 25 images and compute the percentage of images in which the target celebrity is still recognizable.

**Specificity:** The values are obtained in the same way as for the Efficacy, but for the 100 non-target celebrity names.

**Composite Score.** We compute a composite score that balances erasure efficacy and retention specificity, defined as the harmonic mean of  $(1 - \text{Efficacy})$  and Specificity, providing a single measure of unlearning quality:

$$H_o = \frac{2}{(1 - \text{Acc}_e)^{-1} + (\text{Acc}_s)^{-1}}, \quad (7)$$

where  $\text{Acc}_e$  denotes efficacy and  $\text{Acc}_s$  specificity, and a higher value of  $H_o$  indicates a better trade-off between erasing the target celebrities and retaining the remaining ones.